Taylor & Francis
Taylor & Francis Group

Modelling and analysis of hydraulic step-down switching converters

Victor J. De Negri[a]*, Marcos P. Nostrani[a], Pengfei Wang[b] , D. Nigel Johnston[b] and Andrew Plummer[b]

[a]*Department of Mechanical Engineering, LASHIP, Federal University of Santa Catarina, Trindade, Florianópolis, SC 88040-900, Brazil;* [b]*Department of Mechanical Engineering, PTMC, University of Bath, Claverton Down, Bath BA27AY, UK*

In this study, a steady state analysis of step-down converter systems, considering the load losses in the inertance tube and switched valve, is presented. The model describes the behaviour of the average load pressure as a function of the pulse-width modulated duty cycle. The steady state expressions for the load flow rate, high and low supply flow rates, and system efficiency are also discussed. A system prototype was developed and tested to evaluate the model accuracy. The system parameters (e.g. tube diameter and length and switching frequency) were analysed to predict the best system configuration. The study describes how the system efficiency is influenced by these parameters. The model presented allows the ideal parameter combination for maximum efficiency to be determined. It can be used for the preliminary design of switching converters, and a further time or frequency analysis can be performed for system optimization.

Keywords: digital hydraulics; hydraulic switching converter; hydraulic valve; PWM switched valve

1. Introduction

Recently, the energy efficiency of hydraulic systems has been an important research topic in the fluid power community. Consequently, industry and academia have proposed alternative high efficiency component and circuit designs.

It is known that the main cause of the low energy efficiency of hydraulic systems, often less than 50%, is the extensive use of valves to throttle the flow, limit /reduce the hydraulic pressure, or reduce the flow rate in a hydraulic circuit.

In this context, there are two approaches being studied in order to achieve more efficient systems: analog control of pumps and motors and digital hydraulics. The first one includes variable displacement pumps and motors (Eggers *et al.* 2005) and fixed or variable pumps driven by variable speed electrical motors (Willkomm *et al.* 2014).

Research on digital hydraulic systems has intensified since the beginning of the twenty-first century (Scheidl *et al.* 2011). An example is the digital piston pump in which the on/off valves are individually connected to each piston (Rampen 2006, Linjama 2011, Karvonen *et al.* 2014). Multichamber cylinders controlled by parallel valves switching different pressure sources (Heitzig and Theissen 2011, Heitzig *et al.* 2012) and fixed displacement pumps and motors with output/input flow rates controlled by pulse-modulated valves or parallel valves (Linjama 2011) are examples of hydraulic components with on/off valves connected to their ports.

These system configurations can be considered as digital energy conversion units. Moreover, new arrangements of valves are being studied for interconnecting conventional pumps and actuators to replace the directional proportional valves or flow control valves. The digital flow control unit combines restrictions with on/off valves (Linjama 2011). Another alternative is the switched-reactance hydraulics that comprises a circuit composed of at least a pulse-width modulated (PWM) valve and a tube of relatively long length and small diameter.

Switched-reactance hydraulics was studied by Brown in the 1980s (Brown 1987, Brown *et al.* 1988). This type of hydraulic control is based on the cyclical acceleration and deceleration of fluid or a solid inertance using PWM. There is a direct analogy of this hydraulic system with electrical switched power converters used extensively nowadays. The flow or pressure control of the switched-reactance hydraulics is not dissipative, thus high energy efficiency is expected. However, as shown in this study and in De Negri *et al.* (2014), the valve and tube load losses can reduce the efficiency considerably. Brown (1987) noted efficiency drop related to tube viscous friction but he did not model it. Brown *et al.* (1988) and Manhartsgruber *et al.* (2005) presented dynamic models of switching hydraulic systems including friction. In those papers the objective was not to present a steady-state lumped parameter model as discussed in the present study.

Scheidl *et al.* (2008) presented an overview of switching control principles, including the buck converter (step-down transformer) investigated by Brown (1987). Brown *et al.* (1988), Hettrich *et al.* (2009), Wang *et al.* (2011a), and Wang *et al.* (2011b) presented time responses using lumped parameter modelling where the tube and/or valve load loss were included. Manhartsgruber *et al.*

---

*Corresponding author. Email: victor.de.negri@ufsc.br

(2005) presented a frequency and time-domain model of a step-down circuit. Brown (1987), Kogler and Scheidl (2008), and Johnston (2009) showed steady-state equations for average-values of pressure and flow rates not considering load losses.

Kogler and Manhartsgruber (2009) presented an expression for the average flow rate through the tube, taking into account the tube resistance, but the dependence of the output pressure and other flow rates through the system on the tube resistance and switching frequency was not the focus in the study. Dynamic time responses of a linear hydraulic drive controlled by a buck converter are analysed. Wang *et al.* (2011b) studied a step-down system driving a hydraulic system using a flywheel. They deduced an expression for the average load pressure as a function of viscous friction losses and the mechanical efficiency of the motor. However, they did not take these losses into account in their theoretical and experimental analyses.

In this study, a steady-state lumped parameter modelling of a step-down transformer comprising one three-port on/off valve and an inertance tube is presented. The modelling strategy is an extension of a previous study by current authors for a step-up configuration.

The model is experimentally validated and can be used for the steady-state analysis and design of this type of device in general. Based on the presented equations, the performance related to energy efficiency is analysed. The determination of the best values for the switching frequency, the tube diameter and tube length is also discussed.

This paper is organized as follows. In Section 2, the fundamentals of the step-down converter are described. In Section 3, the hydraulic step-down converter is modelled, including the resistance associated with the tube and switching orifices. Section 4 presents the experimental setup and the system parameters. In Section 5, the experimental and theoretical results for different switching times are compared to confirm the model validity. Section 6 presents an analysis of the system parameters (e.g. tube diameter and length and switching frequency) and describes how the system efficiency is affected. Section 7 summarizes the conclusions of the study.

2. Step-down converter

Figure 1 shows the fundamental circuit of a hydraulic step-down switching converter and its corresponding electrical system. A single solenoid spring return directional valve is driven by a PWM signal, to modulate the time at which each flow path remains active. A hydraulic tube is connected to the valve port A, which introduces the inertance (L_t) and also the hydraulic resistance (R_t) and capacitance (C_t) effects. As will be discussed in the following sections, the resistance has a significant effect on the system performance; therefore, it is included in the mathematical modelling.
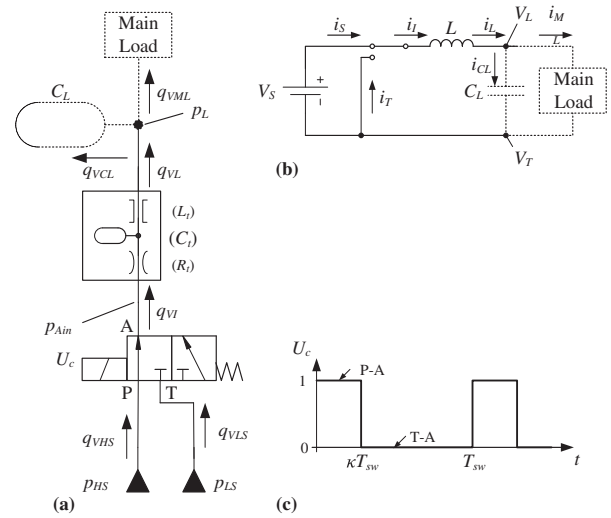

Figure 1. Step-down converter: (a) hydraulic circuit; (b) electrical circuit; (c) PWM input signal.

As can be seen in Figure 1, when the flow path P-A is active, the internal pressure (p_{Ain}) tends to increase. Consequently, the fluid accelerates through the tube. When the valve switches to the other position, the internal chamber is connected to the port (T). However, the fluid momentum causes the fluid to continue to move through the tube, drawing the fluid from the port (T) despite the adverse (low to high) pressure gradient between the low pressure supply port (T) and the load output. When the duty cycle (κ) is equal to 100% (P-A and T are blocked), the load pressure (p_L) is ideally equal to both p_{Ain} and the high supply pressure (p_{HS}). When $\kappa = 0\%$, the T port is connected to A, and P is blocked such that p_L and p_{Ain} are equal to the low supply pressure (p_{LS}). Ideally, the load pressure (p_L) can be modulated from the low supply pressure value to the high supply pressure value, proportional to the duty cycle.

The step-down circuit can be analysed as a pressure regulator in the same manner that an electrical converter is a voltage regulator. Therefore, the average flow rate consumed by the load is a perturbation signal for the system and, as discussed in the following sections, it reduces the regulated pressure.

3. Step-down PWM valve modelling

Assuming that the load capacitance (C_L) in the step-down circuit shown in Figure 1 is sufficiently high for the load pressure (p_L) to be considered constant. Then the switching circuit can be analysed separately from the main load system.

Therefore, the step-down system can be modelled on the basis of the circuit shown in Figure 2, where Δp corresponds to the pressure drop through both the directional valve and inertance tube and q_{VI} is the inertance tube flow rate.
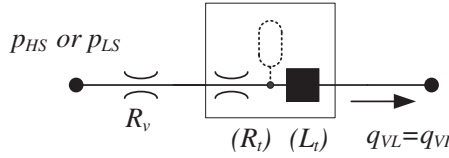
Figure 2. Step-down fundamental hydraulic circuit with resistances.

As previously stated, in the step-down circuit, there are two different valve flow paths at the tube upstream that are switched alternately. These consequently connect the high supply (p_{HS}) or the low supply (p_{LS}) lines to the tube. Assuming that both valve flow paths have the same resistance (R_v), the circuit model is given by

$$\frac{L_t}{R_{eq}}\frac{dq_{VI}}{dt} + q_{VI} = \frac{1}{R_{eq}}\Delta p, \qquad (1)$$

where $\Delta p = p_{HS} - p_L$ for $0 \leq t \leq \kappa T_{sw}$, $\Delta p = p_{LS} - p_L$ for $\kappa T_{sw} \leq t \leq T_{sw}$, and $R_{eq} = R_v + R_t$.

The tube inertance is determined by

$$L_t = \frac{4\rho l_t}{\pi d_t^2} \qquad (2)$$

and the tube resistance for a laminar flow, calculated by

$$R_t = \frac{128\rho l_t v}{\pi d_t^4}. \qquad (3)$$

Based on the approach by Millmann and Taub (1965) for electric circuits, the time response of this hydraulic system for a square-wave input can be expressed by

$$q_{V1}(t) = \frac{p_{HS} - p_L}{R_{eq}} + \left(q_{V1}(0) - \frac{p_{HS} - p_L}{R_{eq}}\right)e^{-t/\tau} \qquad (4)$$
for $0 \leq t \leq \lambda T_{sw}$

and

$$q_{V2}(t) = \frac{p_{LS} - p_L}{R_{eq}} + \left(q_{V2}(\kappa T_{sw}) - \frac{p_{LS} - p_L}{R_{eq}}\right)e^{-(t-\kappa T_{sw})/\tau}$$
for $\kappa T_{sw} \leq t \leq T_{sw}$,

$$\qquad (5)$$

where $\tau = L_t/R_{eq}$ is a time constant.

Figure 3(a) shows the graphical representation of these functions and their specific values at 0, κT_{sw} and T_{sw}. As demonstrated by Millmann and Taub (1965), the average output value (q_{VI}) is equal to the average input value (Δp) multiplied by the steady-state gain for an entire period. Figure 3(b) presents a specific condition where the duty cycle is equal to 50%.

Calculating the high pulse flow rate at $t = \kappa T_{sw}$, i.e. ($q_{V1}(\kappa T_{sw}) = q_{V1}(\kappa T_{sw})$) and the low pulse flow rate at $t = T_{sw}$, i.e. ($q_{V2}(T_{sw}) = q_{V1}(0)$), the amplitude of the flow wave can be expressed by

$$\Delta q_{VI} = \Delta q_{V1} = \Delta q_{V2} =$$
$$\frac{(1 - e^{-(1-\kappa)T_{sw}/\tau} - e^{-\kappa T_{sw}/\tau} + e^{-T_{sw}/\tau})}{(1 - e^{-T_{sw}/\tau})} \cdot \frac{(p_{HS} - p_{LS})}{R_{eq}}.$$
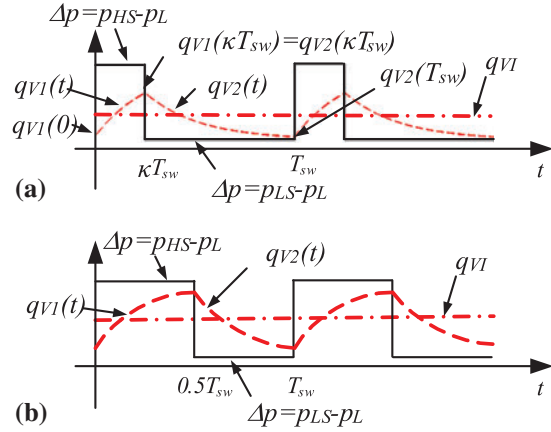
$$\qquad (6)$$

Figure 3. Inertance tube response for a square wave (system with resistance): (a) general response; (b) response for $\kappa = 0.5$.

According to De Negri *et al.* (2014), for the step-up converter, the average flow rate through the inertance tube (q_{VL}), average high supply flow rate (q_{VHS}), and average low supply flow rate (q_{VLS}), respectively, can be obtained from Equations (4) and (5) to give

$$q_{VL} = \frac{(p_{LS} - p_L)(1 - \kappa)}{R_{eq}} + \frac{(p_{HS} - p_L)\kappa}{R_{eq}}, \qquad (7)$$

$$q_{VHS} = \frac{\tau(1 - e^{-T_{sw}(1-\kappa)/\tau})(1 - e^{-T_{sw}\kappa/\tau})(p_{LS} - p_{HS})}{(1 - e^{-T_{sw}/\tau})R_{eq}T_{sw}}$$
$$+ \frac{(p_{HS} - p_L)\kappa}{R_{eq}},$$

$$\qquad (8)$$

and

$$q_{VLS} = \frac{\tau(1 - e^{-T_{sw}(1-\kappa)/\tau})(1 - e^{-T_{sw}\kappa/\tau})(p_{HS} - p_{LS})}{(1 - e^{-T_{sw}/\tau})R_{eq}T_{sw}}$$
$$+ \frac{(p_{LS} - p_L)(1 - \kappa)}{R_{eq}}.$$

$$\qquad (9)$$

According to Equation (7), the output flow rate of the step-down converter depends on supply pressures and duty cycle and it is influenced by the tube and valve load losses. Moreover, the system can be observed as a pressure controller, the load flow rate being a disturbance input and Equation (7) can be rewritten as

$$p_L = (p_{HS} - p_{LS})\kappa + p_{LS} - q_{VL}R_{eq}. \qquad (10)$$

Equation (10) shows that the load pressure in a step-down converter does not depend on the switching period, and has a linear behaviour with respect to the duty cycle. However, the flow rate required by the system causes a load loss in the tube and switching valve, which reduces the regulated pressure. Equation (10), ignoring the last term on the right-hand side, corresponds to the ideal step-down converter (Brown 1987, Kogler and Scheidl 2008, Johnston 2009).

Assuming average values of pressures and flow rates over a switching period, the energy efficiency under steady state conditions can be expressed by

$$\eta = \frac{p_L q_{VL}}{p_{HS} q_{VHS} + p_{LS} q_{VLS}}. \tag{11}$$

Using Equations (5)–(8), the efficiency can be written as a function of system inputs (q_{VL}, p_{HS}, p_{LS}, κ) and parameters (T_{sw}, R_{eq}, τ ($\tau = L_t/R_{eq}$)), as follows

$$\eta = \frac{q_{VL}[p_{HS}\kappa + p_{LS}(1-\kappa)] - q_{VL}^2 R_{eq}}{\dfrac{(p_{HS}-p_{LS})^2 \psi}{R_{eq}} + q_{VL}[p_{HS}\kappa + p_{LS}(1+\kappa)]}, \tag{12}$$

where

$$\psi = \kappa(1-\kappa) - \frac{\tau(1 - e^{-T_{sw}(1-\kappa)/\tau})(1 - e^{-T_{sw}\kappa/\tau})}{(1 - e^{-T_{sw}/\tau})T_{sw}}. \tag{13}$$

The function $\psi(\kappa, T_{sw}, \tau)$ does not include supply pressures and load flow rate and, therefore, it is independent of the power controlled by the converter. Furthermore, since the switching period does not occur in any other term of Equation (12), its influence on the efficiency can be analysed exclusively by this function. Numerical results are discussed in Section 6.

Neglecting the valve load loss ($R_v = 0$), Equation (12) can be derived in relation to the tube length and equalling it to zero to determine the tube length for the maximum efficiency, that is:

$$l_t = \frac{-f_1 \psi + \sqrt{(f_1 \psi)^2 + f_2}}{f_3} \pi d_t^4, \tag{14}$$

where

$$f_1 = 2q_{VL}^2 (p_{HS} - p_{LS})^2,$$

$$f_2 = 4q_{VL}^4 (p_{HS} - p_{LS})^2 [(p_{HS}\kappa + p_{LS})^2 - p_{LS}^2 \kappa^2], \text{ and}$$

$$f_3 = 256 q_{VL}^3 \rho v [p_{HS}\kappa + p_{LS}(1 + \kappa)].$$

Equations (7)–(14) presented above model analytically the steady state average behaviour of a step-down converter. They are suitable for system dimensioning from the point of view of output flow or pressure performance and energy efficiency.

4. Experimental system setup

A hydraulic circuit (Figure 4) was implemented for the experimental study. The circuit comprises four turbine flow meters (S1, S6, S8, and S9), four strain gauge pressure transducers (S3, S4, S5, and S7), and a thermocouple (S2). The accumulators (Ac2 and Ac3) were used to keep the high and low supply pressures as constant as possible and the accumulator (Ac1) was used to absorb pressure peaks. The nominal accumulator volumes are one liter and the preload pressures are equal to 80% of the nominal working pressure on each line. The role of

the directional valve shown in Figure 1(a) is performed by a directional proportional valve, V1, (Parker D1FPE50MA9NB01) whose parameters are presented in Table 1. The equivalent resistance was calculated from the experiments, as shown in De Negri *et al.* (2014).

The inertance tube (T1) has internal diameter (d_t) of 7.1 mm and length (l_t) of 1.7 m. The hydraulic fluid has density (ρ) of 870 kg/m³, kinematic viscosity (v) of 32×10^{-6} m²/s and is assumed to have an effective bulk modulus (β_e) of 1.6×10^9 Pa. Using the Equation (2), the tube inertance (L_t) is 3.75×10^7 kg/m⁴. The tube capacitance ($C_t = V_t/\beta_e$) is 4.23×10^{-14} m³/Pa and the load capacitance is approximately 10×10^{-11} m³/Pa. The tube measured resistance (R_t) is 1.67×10^9 Pa s/m³, resulting on the equivalent resistance (R_{eq}) of the valve and tube as 5.55×10^9 Pa s/m³.

5. Theoretical and Experimental Results

5.1. Introduction

The equations presented in Section 3 describe the steady-state behaviour of a step-down PWM valve, i.e. assuming that the inputs duty cycle and average load flow rate are constant as well as the switching frequency and high and low supply pressures. The resulting response corresponds to the average values of a time period.

To validate this model, experiments were conducted using the setup described in Section 4. Switching periods of 125 ms ($f_{sw} = 8$ Hz), ($f_{sw} = 16$ Hz), and 25 ms ($f_{sw} = 40$ Hz), were used, taking into account the valve settling time shown in Table 1. For the first two periods, the spool achieved total displacements on the boundary duty cycles of 10 and 90%. As shown below, for 25 ms, the valve responded for duty cycles between 30 and 70%.

The experiments were conducted for different duty cycles while keeping the average load flow rate constant, which was adjusted by valve V2 (Figure 4). The average high supply pressure (p_{HS}) was adjusted to 2.4 MPa, and the values of the average low supply pressure (p_{LS}) during the tests are shown in Table 2.

5.2. Switching period of 125 ms

Figure 5 presents the load pressure controlled by the step-down converter as a function of the duty cycle and load flow rate. The switching frequency (f_{sw}) is 8 Hz ($T_{sw} = 125$ ms). As one can see, the tube and valve load losses have a large influence on the system performance, and thus, the regulated pressure is reduced as the load flow rate increases. In this figure, and in the following ones, the lines correspond to the theoretical results according to the equations presented in Section 3, whereas the points correspond to the experimental results.

The experimental values in Figure 5 demonstrate that the load pressure has a linear dependence on the duty cycle and its magnitude depends on the load flow rate (q_{VL}), as denoted by Equation (10). Since a linear, rather than a square root, function of the flow rate with the
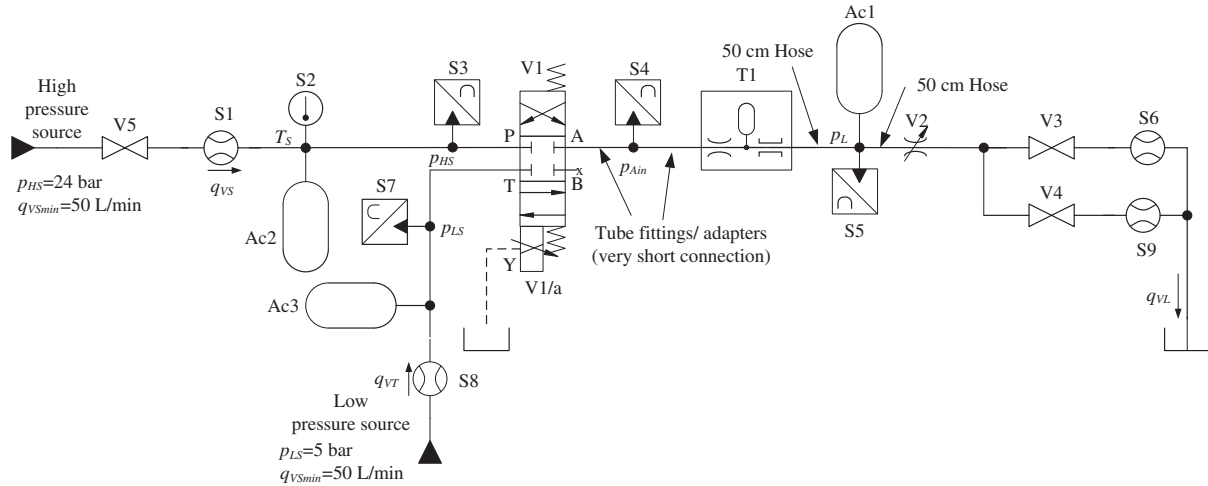
Figure 4. Hydraulic circuit diagram.

Table 1. Parameters of the proportional valve.

Nominal flow rate (q_{Vn})	0.67 L/s (40 L/min) @ $\Delta p_p = 3.5$ MPa [b]
Valve resistance (R_v)	3.88×10^9 Pa.s/m³@ $U_c = \pm U_{cn}$[a]
Settling time (t_s)	3.5 ms @ $U_c = 0 \rightarrow +100\%$[b]
	6.25 ms @ $U_c = -100 \rightarrow +100\%$[a]
Natural frequency (ω_n)	120 Hz @ 90° ($U_c = \pm 90\%$)[b]

[a]Experimental data.
[b]Catalogue data.

valve pressure drop is assumed, the theoretical results differ from experimental ones as the flow rate through the valve increases. The valve characteristic curves are shown in De Negri *et al.* (2014).

Furthermore, negative pressures can be determined numerically, but they do not occur in practice because of the air solubility and/or fluid vaporization at such conditions. Therefore, the achieved minimal value of the duty cycle that results in a load pressure equal to the low supply pressure increases as the flow rate to the load system increases.

Figures 6 and 7 present the average high and low supply flow rates, respectively, where the experimental points confirm the model prediction.

5.3. Switching periods of 62.5 and 25 ms

Theoretical and experimental results for the same conditions as those described in the Section 5.1 were obtained
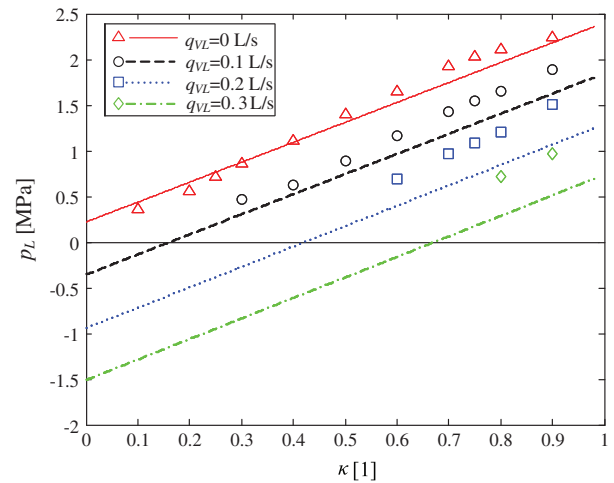

Figure 5. Load pressure vs. duty cycle for 8 Hz (Equation (10)).

using switching frequencies (f_{sw}) of 16 Hz ($T_{sw} = 62.5$ ms) and 40 Hz ($T_{sw} = 25$ ms).

Figure 8 presents the load pressure for 16 Hz. At this frequency the pulse time at 10 and 90% is 6.25 ms, which is equal to the valve settling time. As the valve dynamic response is not considered in the modelling, it is possible to conclude that the valve opening transient does not introduce substantial load losses as the valve achieves its full opening.

Table 2. Average low supply pressures.

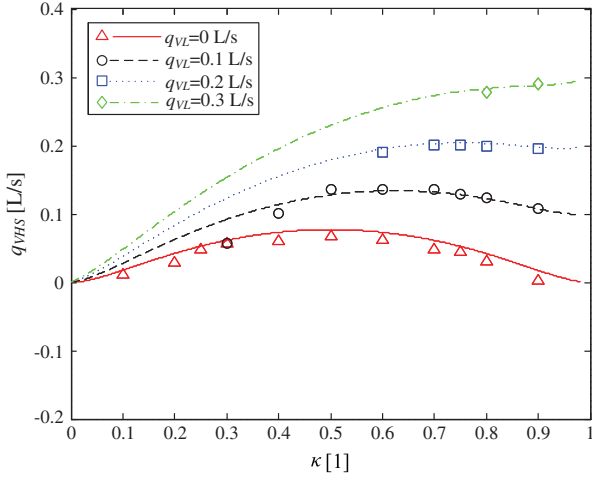|	Average low supply pressure		
Load flow rate	For $T_{sw} = 125$ ms	For $T_{sw} = 62.5$ ms	For $T_{sw} = 25$ ms
0 L/s	0.22 MPa	0.25 MPa	0.23 MPa
0.1 L/s	0.20 MPa	0.21 MPa	0.22 MPa
0.2 L/s	0.17 MPa	0.19 MPa	0.20 MPa
0.3 L/s	0.15 MPa	0.19 MPa	0.16 MPa

Figure 6. High supply flow rate vs. duty cycle for 8 Hz (Equation (8)).
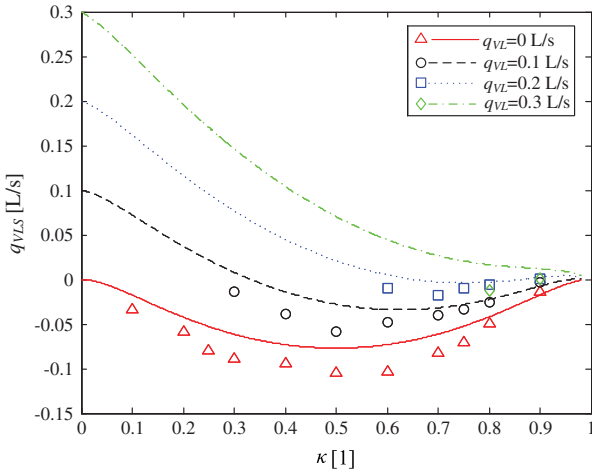

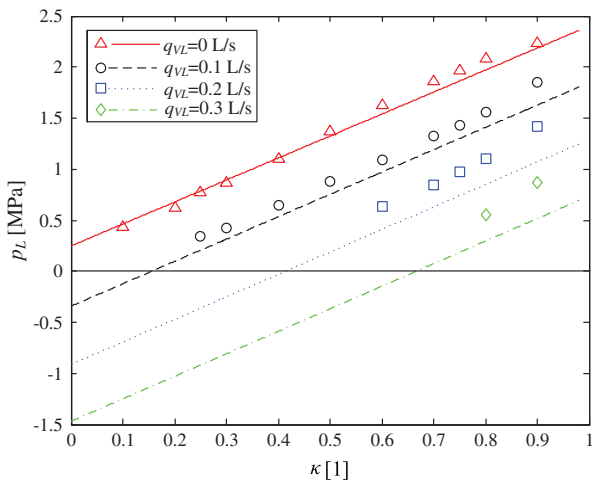Figure 7. Low supply flow rate vs. duty cycle for 8 Hz (Equation (9)).

Figure 8. Load pressure vs. duty cycle for 16 Hz (Equation (10)).

The good proximity of the experimental points in relation to the theoretical curves corroborates the model adequacy.

Experimental and numerical results using a switching frequency (f_{sw}) of 40 Hz ($T_{sw} = 25$ ms) are shown in Figures 9–11. As can be observed, the experimental curve shapes are close to the ones predicted by the model, but some points are dispersed.

For 40 Hz, the valve does not respond fast enough, particularly, for boundary duty cycles. For example, Figure 12(a) shows the dynamic valve spool position for a duty cycle of 40% when the valve achieves the final position at each pulse. However, for a duty cycle of 90% (Figure 12(b)), the valve is unable to fully connect ports A to T. Consequently, the load pressure and the high supply flow rate are higher, whereas the low supply flow rate is lower than the theoretical values (Figures 9–11).

Generally, for lower duty cycles, when the valve does not achieve full opening of P to A and a full closing to port T, the regulated pressure and high supply flow rate tend to be lower than expected. Conversely, for higher duty cycles, the regulated pressure is higher and the low supply flow rate is lower than expected.

6. Parameter optimization

6.1. Switching frequency

As it could be observed in the previous section, the theoretical model predicts very well the steady state average response as the switching valve can achieve full opening and closing during a time period.

Therefore, the equations presented in Section 3 can be used for the analysis of the influence of the step-down parameters in the energy efficiency as presented hereinafter. Simulation results are based on the operational conditions shown in Table 3.
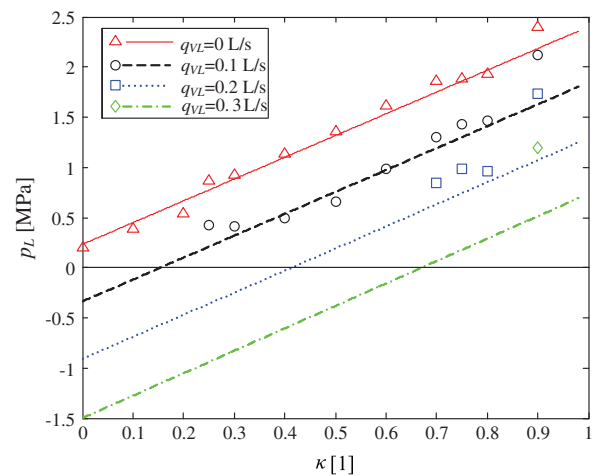

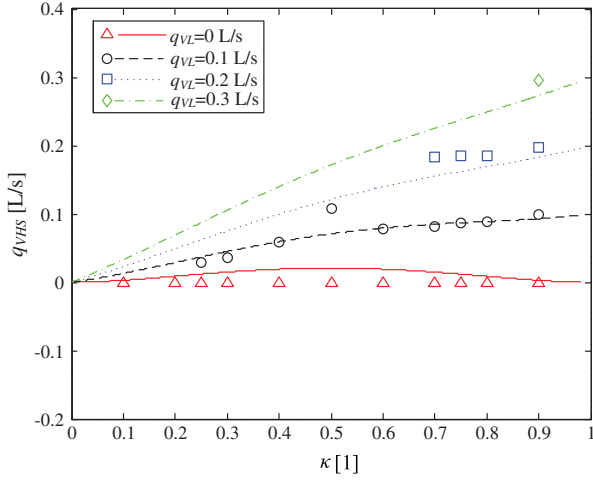Figure 9. Load pressure vs. duty cycle for 40 Hz (Equation (10)).

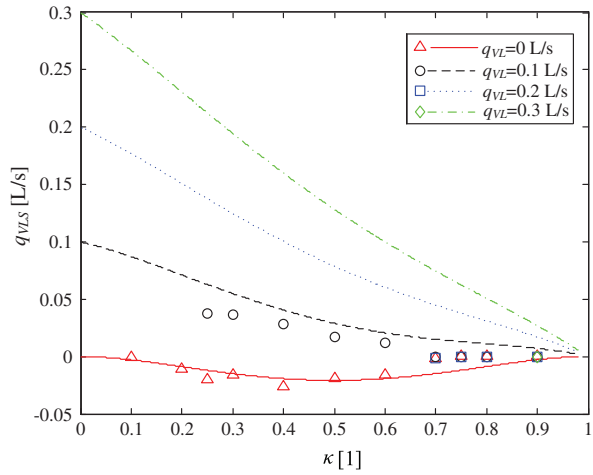Figure 10. High supply flow rate vs. duty cycle for 40 Hz (Equation (8)).

Figure 11. Low supply flow rate vs. duty cycle for 40 Hz (Equation (9)).

Figure 12. Valve response (a) $\kappa = 0.4$, (b) $\kappa = 0.9$.

Table 3. Operational conditions used in simulations.

High supply pressure (p_{HS})	12 MPa
Low supply pressure (p_{LS})	0.3 MPa
Load flow rate (q_{VL})	2×10^{-4} m^3/s
Fluid properties	According Section 4

Figure 13. Efficiency vs. duty cycle for different switching frequencies (Equation (11)).

As shown in Sections 3 and 5, the switching frequency has a significant influence on the average high and low supply flow rates for intermediate duty cycles. Consequently, the switching frequency directly influences the step-down efficiency.

Considering a tube of 6 m of length and 7 mm of internal diameter, Figure 13 shows how the efficiency varies with different switching frequencies according to Equation (11).

As shown in Figure 13, as the switching frequency increases, the efficiency increases too for intermediate values of the duty cycle. This effect can be understood by analysing Equations (12) and (13).

Figure 14 shows that $\Psi(\kappa, T_{sw}, \tau)$ (Equation (13)) is a symmetric function with respect to κ and the minimal values occur at the boundaries. The function magnitude decreases as f_{sw} and τ increase and, consequently, the efficiency increases (according to Equation (12)). Unlike for
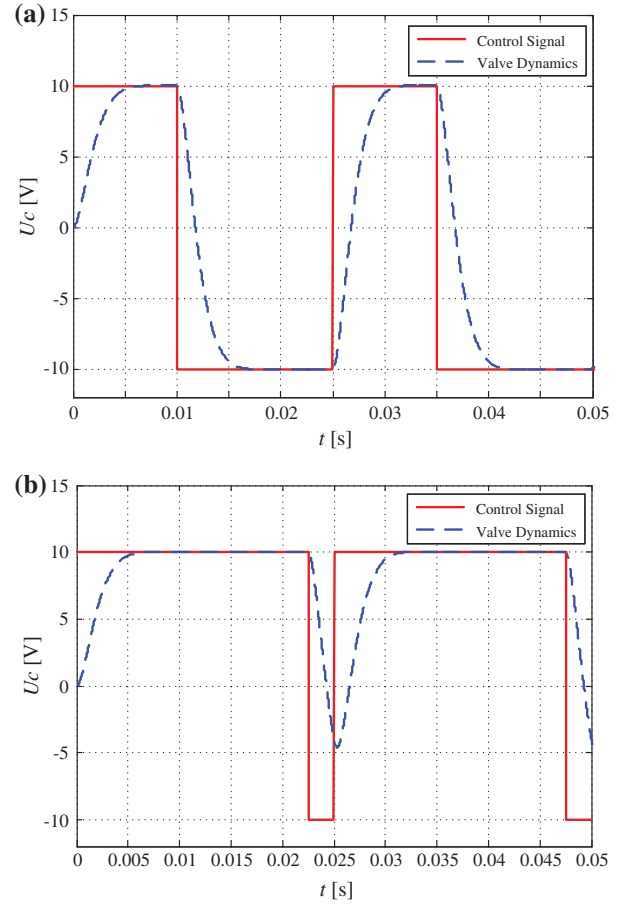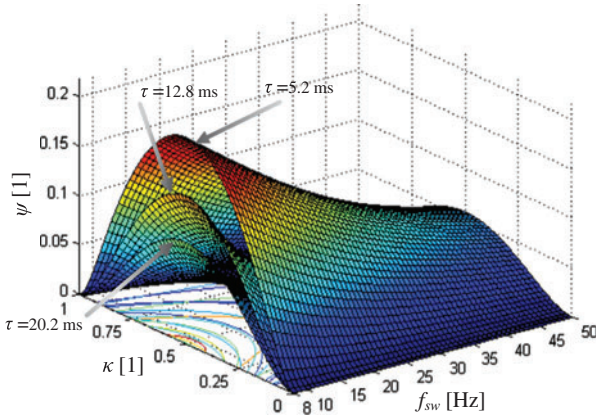
Figure 14. Function Ψ vs. switching frequency and duty cycle for different time constant values (Equation (13)).

6.2. Diameter and length

As discussed previously, the step-down converter efficiency (Equation (11) or Equations (12) and (13)) depends on the system parameters, i.e. the tube inertance and resistance, valve resistance, and switching period. Moreover, the tube inertance (Equation (2)) and resistance (Equation (3)) depend on the diameter and length. Therefore, the system performance can be evaluated according to these two elementary parameters.

The following analysis considers a tube diameter between 5 and 20 mm. The minimal tube length is calculated by $l_t = 138d_t$ for laminar flow (Fox *et al.* 2011). The operational conditions are according to Table 3 and the switching frequency is 40 Hz ($T_{sw} = 25$ ms). The duty cycle is adjusted to 0.5, in which the influence of the parameters in the system performance is more significant (Figures 13 and 14).

Figure 16 exemplifies the use of Equation (11) to predict how the different combinations of tube diameter and length affect the step-down efficiency. The results demonstrate that for diameters smaller than 10 mm there is an optimum tube length that provides maximum efficiency. For greater diameters, the reduction in the efficiency is not significant from the length where the maximum efficiency is achieved.

Neglecting the valve resistance, the ordered pairs of tube length and diameter resulting on maximum efficiencies can be determined using Equation (14). Figures 17 shows that greater diameter requires longer tube to achieve the maximum system efficiency.

The influence of the valve resistance on the tube sizing and the step-down converter efficiency can be evaluated using Equation (12). Starting from $R_v = 0$, the maximum efficiency was determined as a function of the valve resistance and for different tube diameters. As can be seen, to achieve the maximum efficiency as possible, the tube length must be increased from that obtained

the switching period, the tube and valve resistances are present in other terms of Equation (12) and, therefore, their influence cannot be only based on the Ψ behavior.

According to Figures 13 and 14, frequencies of 40 Hz ($T_{sw} = 25$ ms) and 50 Hz ($T_{sw} = 20$ ms) result in very similar efficiencies. Figure 15 shows the efficiency for switching frequencies from 8 Hz ($T_{sw} = 125$ ms) to 150 Hz ($T_{sw} = 6.6$ ms) which points out that the subsequent frequency increase from 50 Hz does not contribute significantly to the system performance.

Therefore, the efficiency is not significantly improved using switching valves with extremely high response time. For example, at 50 Hz, valves with settling times of 2 ms are qualified for operation with duty cycles between 10 and 90%. Valves with such dynamic performance are being developed by research institutes (Winkler *et al.* 2008, 2010, Uusitalo *et al.* 2010). Commercial valves up to 10 ms are reported by (Murrenhoff, 2003, Linjama and Vilenius 2008).
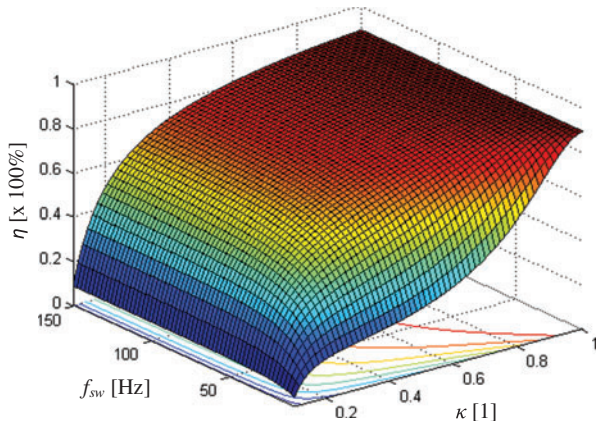

Figure 15. Efficiency for switching frequencies from 8 to 150 Hz (Equation (11)).
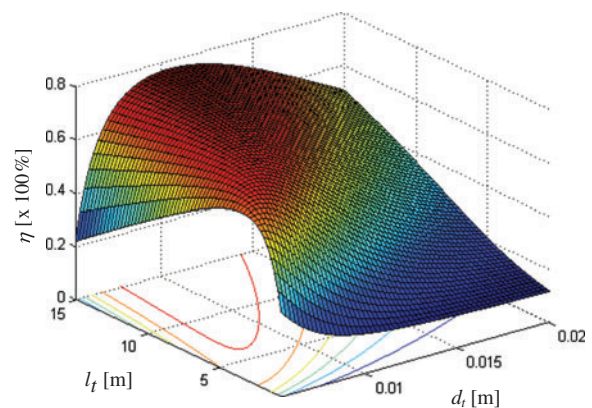

Figure 16. Step-down efficiency vs. tube diameter and length for $\kappa = 0.5$ (Equation (11)).
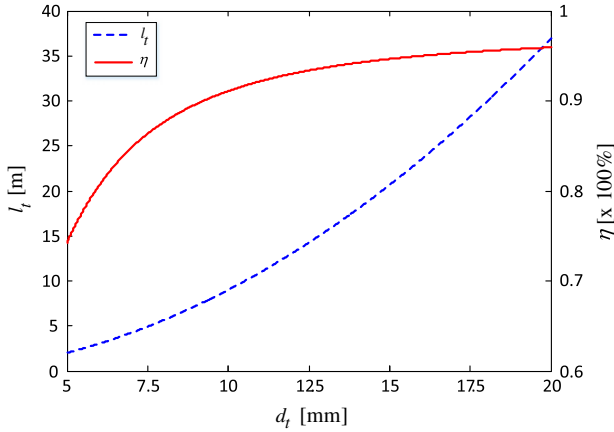
Figure 17. Tube length vs. diameter for maximum efficiency (Equation (14)).

using Equation (14) (Figure 17). However, the higher the valve resistance, the lower the efficiency, as expected.

The analysis presented in this section does not take into account the resonance frequencies of the tube and the excitation that can be caused by the valve switching. Considering the fluid parameters presented in Section 4, the first resonant frequency for a tube length of 6 m with open-open boundary conditions is 113, and 45.2 Hz for 15 m, for example. Thus, the longer the tube, the greater the possibility of exciting the resonance, resulting in undesirable noise and vibration.

Furthermore, when resonance occurs, the flow behaviour will be far from that represented in Figure 3 and, consequently, the modelling presented in this paper will not be valid.

As an example of tube sizing of a step-down converter working on the operational conditions shown in Table 3, a tube of 7 mm diameter was chosen. This tube size can be easily conformed in spiral, reducing the occupied space and resulting on a feasible step-down
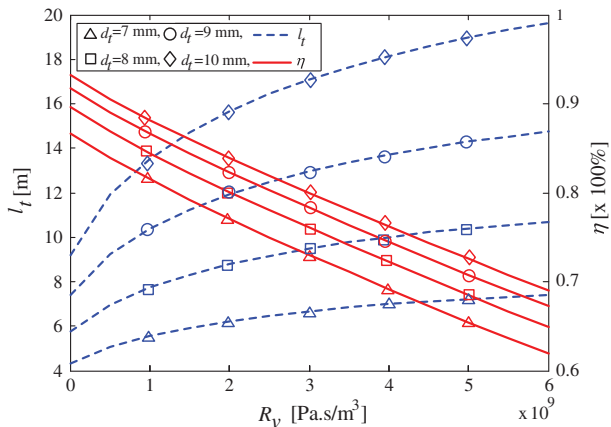

Figure 18. Tube length vs. valve resistance for maximum efficiency (Equation (12)).

converter. The step-down converter comprises a valve as described in Table 1 ($R_v = 3.88 \times 10^9$ Pa s/m^3). According to Figure 18, the tube length for maximum efficiency is 6.95 m and the corresponding efficiency equal to 0.696. Based on that, a standard 6 m length tube was chosen since the corresponding efficiency of 0.693 (calculated by Equation (12)) is very similar to the tube using the ideal length.

7. Conclusions

A steady state lumped parameter model of the step-down PWM valve, which is of interest for the analysis and design of new systems based on the switched inertance principle is presented. Using the model that includes linear resistance, theoretical and experimental results show that it is possible to predict the average value of the controlled pressure and flow rates at the step-down converter ports.

Therefore, despite the flow-pressure nonlinearity and the limited time response of the switching valve as well as the pressure wave propagation in the inertance tube, the presented linear model describes very well the global behaviour of step-down switching converters.

The dynamic behaviour of switching converters is complex. Several phenomena occur such as fluid compressibility in the internal chambers and wave propagation through the tube. Determining the effectiveness of the system design on the basis of dynamic simulation is straightforward. In this context, the proposed model can be used for the preliminary design of switching converters, and a further time or frequency analysis can be performed for system optimization.

According to the equations presented in this paper, in the step-down converter, the average high and low supply flow rates depend on the PWM signal period, resistance, inertance and the average load flow rate, but the load pressure does not depend on the switching period. A study of the parameters of the inertance tube (diameter and length) and switching period was conducted; thus, the presented equations can be used to predict the best combination for the maximum efficiency in each case.

The study presented in this paper is valid when the resonance frequency of the tube is not excited by the switching valve. Therefore, it is suggested the switching frequency to be lower than the tube first resonant frequency.

The switching frequency directly influences the system efficiency; however, for high values, the variation in efficiency is insignificant. The valve dynamics must be sufficiently high to operate with duty cycles between 10% and 90%. Therefore, using this model, it is possible to determine the ideal parameter combination for maximum efficiency and time response of the valve.

Nomenclature

C_t	Tube capacitance	[m^3/Pa]
C_L	Load capacitance	[m^3/Pa]
d_t	Tube diameter	[m]
f_1	Auxiliary function	[m^4 kg^2/s^6]
f_2	Auxiliary function	[m^8 kg^4/s^{12}]
f_3	Auxiliary function	[m^7 kg^2/s^6]
f_{sw}	Switching frequency	[Hz]
l_t	Tube length	[m]
L_t	Tube inertance	[kg/m^4]
p_{Ain}	Internal working pressure	[Pa]
p_L	Load pressure	[Pa]
p_{HS}	High supply pressure	[Pa]
p_{LS}	Low supply pressure	[Pa]
q_{VI}	Tube flow rate	[m^3/s]
$q_{V1}(t)$	Time-dependent flow rate	[m^3/s]
$q_{V2}(t)$	Time-dependent flow rate	[m^3/s]
q_{VL}	Load flow rate	[m^3/s]
q_{Vn}	Nominal flow rate	[m^3/s]
q_{VCL}	Accumulator load flow rate	[m^3/s]
q_{VML}	Main load flow rate	[m^3/s]
q_{VHS}	High supply flow rate	[m^3/s]
q_{VLS}	Low supply flow rate	[m^3/s]
R_{eq}	Equivalent resistance	[Pa s/m^3]
R_v	Valve resistance	[Pa s/m^3]
R_t	Tube resistance	[Pa s/m^3]
T_{sw}	Switching period	[s]
t	Time	[s]
t_s	Settling time	[s]
U_c	Command signal	[1]
U_s	Spool position voltage	[V]
V_t	Tube volume	[m^3]
Δp	Pressure difference	[Pa]
Δq_{VI}	Tube flow amplitude	[m^3/s]
βe	Effective bulk modulus	[Pa]
η	Energy efficiency	[1]
κ	Duty cycle	[1]
ν	Kinematic viscosity	[m^2/s]
ρ	Fluid density	[kg/m^3]
τ	Time constant	[s]
Ψ	Auxiliary function	[1]
ω_n	Natural frequency	[rad/s]

Disclosure statement

No potential conflict of interest was reported by the authors.

Funding

Notes on contributors

Victor J. De Negri received his D. Eng. degree in 1996, from the Federal University of Santa Catarina (UFSC). In 2010 he took a 7-month sabbatical at PTMC, University of Bath, UK. He has been a Professor at the Mechanical Engineering Department at UFSC since 1995. He is currently the Head of the Laboratory of Hydraulic and Pneumatic Systems (LASHIP). His interest areas include hydraulic components, power generating plants, mobile hydraulics, pneumatic systems and positioning systems.

Marcos P. Nostrani is a Master's Student in the Department of Mechanical Engineering at the Federal University of Santa Catarina (UFSC). His current research is in digital hydraulic systems based on high speed switching valves applied in wind turbines.

Pengfei Wang was a Research Officer in the Department of Mechanical Engineering at the University of Bath. His PhD was also awarded at the same university on hardware in the loop testing of continuously variable transmission (CVT). His research covered fluid power systems like power-assisted steering systems, CVTs, among others.

D. Nigel Johnston is a Senior Lecturer in the Department of Mechanical Engineering at the University of Bath, and teaches computer programming, simulation, numerical analysis and fluid power. His PhD was for research into fluid-borne noise characteristics in hydraulic systems. This work resulted in a new ISO Standard for pump fluid-borne noise testing (ISO 10767-1: 1996). His current research interests include: modelling of the dynamic behaviour of pumps, pipelines and valves, noise in fluid power systems, valve stability, vehicle hydraulics including power-assisted steering systems, flow and pressure transients in aircraft fuel systems.

Andrew Plummer received his PhD degree from the University of Bath in 1991, for research into adaptive control of electrohydraulic systems. He has worked for Rediffusion Simulation on flight simulator control systems, as a lecturer at the University of Leeds, and as R&D manager for Instron. Now Professor of Machine Systems at the University of Bath, and Director of the Centre for Power Transmission and Motion Control.

ORCID

Pengfei Wang http://orcid.org/0000-0001-5897-0569

References

Brown, F.T., 1987. Switched reactance hydraulics: a new way to control fluid power. *Proceedings of the national conference on fluid power*. Chicago: National Fluid Power Association, 25–34.

Brown, F.T., Tentarelli, S.C., and Ramachandran, S.A., 1988. A hydraulic rotary switched-inertance servo-transformer. *Transactions of ASME: journal of dynamic systems, measurement, and control*, 110, 144–150.

De Negri, V.J., Wang, P., Plummer, A., Johnston, D.N., 2014. Behavioural prediction of hydraulic step-up switching converters. *International journal of fluid power*, 15 (1), 1–9.

Eggers, B., Rahmfeld, R., and Ivantysynova, M., 2005. An energetic comparison between valveless and valve controlled active vibration damping for off-road vehicles. *Proceedings of the 6th JFPS international symposium on fluid power*. Tsukuba: Japan Fluid Power System Society.

Fox, R.W., McDonald, A.T., and Pritchard, P.J., 2011. *Introduction to fluid mechanics*, 8th ed. Hoboken, NJ: Wiley.

Heitzig, S. and Theissen, H., 2011. Aspects of digital pumps in closed circuit. *The forth workshop on digital fluid power*, 21–22 September 2011. Linz: ACCM, 39–50.

Heitzig, S., Sgro, S., and Theissen, H., 2012. Energy efficiency of hydraulic systems with shared digital pumps. *International journal of fluid power*, 13, 49–57.

Hettrich, H., Bauer, F., and Fuchshumer, F., 2009. Speed controlled, energy efficient fan drive within a constant pressure system. *Proceedings of the second workshop on digital fluid power*. Linz: ACCM, 62–71.

Johnston, D.N., 2009. A switched inertance device for efficient control of pressure and flow. *Proceedings of the ASME 2009 dynamic systems and control conference – DSCC2009*. Hollywood: ASME.

Karvonen, M., Heikkilä, M., Huova, M. and Linjama, M., 2014. Analysis by simulation of different control algorithms of a digital hydraulic two-actuator system. *International journal of fluid power*, 15 (1), 33–44.

Kogler, H. and Manhartsgruber, B., 2009. Simulation tools and control design for fast switching hydraulic systems. *Proceedings of the second workshop on digital fluid power*. Linz: Tampere University of Technology, 85–93.

Kogler, H. and Scheidl, R., 2008. Two basic concepts of hydraulic switching converters. *Proceedings of the first workshop on digital fluid power*. Tampere: ACCM, 113–128.

Linjama, M., 2011. Digital fluid power-state of the art. *The twelfth Scandinavian international conference on fluid power*, Tampere: Tampere University of Technology.

Linjama, M. and Vilenius, M., 2008. Digital hydraulics – towards perfect valve technology. Technology. *Digitalna Hidravlika*, 14 (2), 138–148.

Manhartsgruber, B., Mikota, G., and Scheidl, R., 2005. Modelling of a switching control hydraulic system. *Mathematical and computer modelling of dynamical systems*, 11 (3), 329–344.

Millmann, J. and Taub, H., 1965. *Pulse, digital, and switching waveforms*. New York: McGraw-Hill.

Murrenhoff, H. 2003. Trends in valve development. *O+P – Ölhydraulik und Pneumatik*, 46 (4), 1–36.

Rampen, W. 2006. Gearless transmissions for large wind turbines–the history and future of hydraulic drives. *Proceedings of the 8th German Wind Energy Conference (DEWEK 2006)*. Bremen: Deutsches Windenergie-Institut.

Scheidl, R., Manhartsgruber, B., and Winkler, B., 2008. Hydraulic switching control – principles and state of the art. *Proceedings of the first workshop on digital fluid power*. Tampere, 31–49.

Scheidl, R., Linjama, M., and Schmidt, S., 2011. Is the future of fluid power digital? *Proceedings of the institution of mechanical engineers. Part I: journal of systems and control engineering*, 226 (6), 721–723.

Uusitalo, J.-P., *et al.*, 2010. Novel bistable hammer valve for digital hydraulics. *International journal of fluid power*, 11 (3), 35–44.

Wang, P., *et al.*, 2011a. The influence of wave effects on digital switching valve performance. *Proceedings of the fourth workshop on digital fluid power*. Linz: ACCM, 10–25.

Wang, F., Gu, L., and Chen, Y., 2011b. A continuously variable hydraulic pressure converter based on high-speed on–off valves. *Mechatronics*, 21, 1298–1308.

Willkomm, J., Wahler, M., and Weber, J., 2014. Process-adapted control to maximize dynamics of displacement-variable pumps. *Symposium on fluid power & motion control*. Bath: University of Bath, 10–12.

Winkler, B., Plöckinger, A., and Scheidl, R., 2008. Components for digital and switching hydraulics. *Proceedings of the first workshop on digital fluid power*. Tampere: Tampere University of Technology, 53–76.

Winkler, B., Ploeckinger, A., and Scheidl, R., 2010. A novel piloted fast switching multi poppet valve. *International journal of fluid power*, 11, 7–14.